ENHANCING SHORE HARDNESS AND RELIABILITY OF SS 316L REINFORCED PMMA NANOCOMPOSITES THROUGH RESIN 3D PRINTING PROCESS OPTIMIZATION

Upender Punia, Ramesh Kumar Garg
•
Department of Mechanical Engineering
Deenbandhu Chhotu Ram University of Science and Technology,
Murthal, Sonipat, Haryana, India - 131039
punia899195@gmail.com, drrkgarg.me@dcrustm.org

Abstract

Over the last ten years, 3D printing has made great progress and expanded its applicability in a number of industries, including dentistry. Dental items including temporary and permanent crowns, bridges, drill guides, and jaw implants may be made using resin 3D printing. To create novel 3D-printable materials and improve their functionality, a lot of research is being done. The shore hardness of 316L-reinforced PMMA nanocomposites for dental applications is examined in this work. Three important process parameters—exposure time (3–5 seconds), layer height (20–40 microns), and post-curing duration (10–30 minutes)—are used to assess the hardness of manufactured specimens. Shore hardness is optimised using Response Surface Methodology (RSM), which yields a maximum shore hardness of 88.90 SHD at 4.75 seconds of exposure time, 30.7 microns of slice height, and 23.2 minutes of post-curing time.

Keywords: Additive manufacturing, Exposure time, Layer height, Post curing time.

I. Introduction

Additive Manufacturing (AM) is a revolutionary manufacturing technique that uses a virtual model to manufacture things in incremental layers [1]. Process parameters are the many settings and variables that are changed in resin 3D printing in order to control the production process and achieve the intended outcomes [2, 3]. AM is used in dentistry to create models for patients and for teaching [4]. Resin 3D printing may be used to create dental items such as bridges, drill guides, jaw implants, temporary and permanent dental crowns, etc. [5, 6]. The dental goods are intricately shaped, personalised for each patient, and built to order. Therefore, 3D printing is ideal for creating dental restorations [7]. These days, CT scans and MRI images may be printed in the ideal form and are readily accessible using software such as mimics. It speeds up and saves money on work [8].

Over the last 10 years, 3D printing's range of applications has significantly expanded, and it is still developing [9]. Universities, government labs, and businesses are all doing a great deal of research to develop novel 3D-printable materials and expand their uses in a variety of industries [10,

11]. The many settings and variables that are changed to control the manufacturing process and achieve the intended outcomes are known as process parameters. The exposure time is the amount of time that the resin material is exposed to UV light at certain wavelengths in order to solidify one layer. It is an important metric since it determines how much the photo-curable resin has polymerised [12]. The effect of exposure period on the elastic modulus has also been investigated by several researchers, and a directly proportional link between the two was discovered. In terms of the resin's degree of curing, the researchers explained the results: a shorter curing time results in less stiffness because of less monomer group convergence. On the other hand, longer light exposure exposes layers to more light energy, which boosts conversion and strengthens the interlayer zone. This leads to increased flexibility and better layer bonding [13, 14]. Layer thickness is the thickness of the layer that is printed all at once. Another name for it is layer height or slice height. Inter-layer zone reinforcement will increase the bonding between the thin layers, increasing the stiffness of the material. Yang et al. claim that although a lower layer height increases printing accuracy, thin layers need more fabrication time, which lowers printing efficiency [15]. The angle formed by the build plate and the product's reference plane is known as the build orientation. The constructed 3D models' stiffness and fracture resistance are impacted by the anisotropy created by their sequential layer-by-layer printing process [16, 17]. The specimens made with a DLP 3D printer show varying tensile strength in various directions, indicating their anisotropic character, according to research by Steyrer et al. and Kebler et al. [18]. Post-curing entails exposing freshly manufactured goods to ultraviolet radiation. In the course of this phase, the polymerisation process proceeds, changing its mechanical properties. Therefore, the amount of UV radiation received, the post-curing temperature, the duration, and the procedures all have a significant impact on the final qualities of the produced components. After curing the samples for half an hour after printing, Staffova et al. examined them using SEM images and discovered that the spaces between the layers were further polymerised. [19]. To remove extra untreated resin from the printed product surface, the freshly resin-printed items must be washed. Additionally, several writers have noted that the mechanical qualities are impacted by washing. Bardelcik et al. used the SLA technology to create samples of acrylic resin. The samples were washed with various solvents, and tensile testing revealed an increased strain [20].

The parametric optimisation of FDM 3D-printed components has been extensively studied, but the parameter optimisation of resin-based 3D printing has received less attention. By examining the hardness of 316L-reinforced PMMA nanocomposites for dental applications, this work makes a unique addition. Shore-D Hardness is the response variable, and three input factors are used to analyse the hardness of manufactured components. To maximise the experimental outcomes, RSM is utilised.

II. Methodology

SolidWorks was used to design the specimens, and an Anycubic Photon Mono X 6K resin-based 3D printer was used to create them using SS 316L-reinforced PMMA nanocomposites. An analogue durometer was then used to assess the hardness of the manufactured test specimens. Using process parameters as input variables and hardness as the response variable, a predictive model was created. Maximum hardness was then attained by optimising the process parameters. Figure 1 shows the approach that was used.

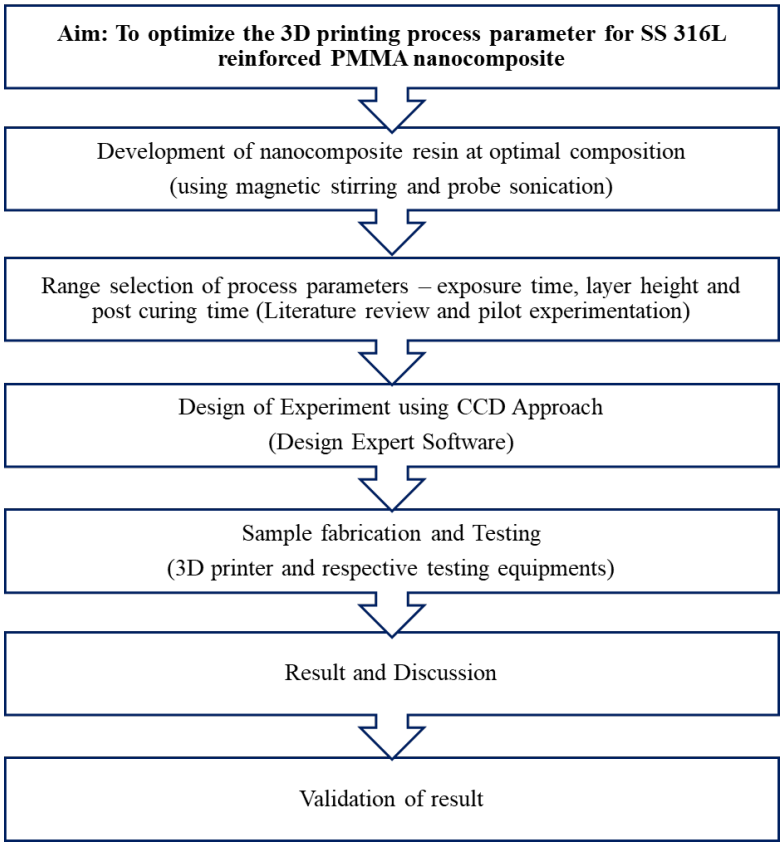

Figure 1: *Methodology adopted*

I. Experimentation

The specimens were developed in accordance with ASTM D2240 for the purpose of assessing hardness. For every resin group, the cuboidal specimens measure 40 × 20 × 6 mm. SolidWorks was used to construct the design, which was then saved in.stl format. After that, this.stl file was sent into Anycubic Photon Workshop, a slicing program that enabled the modification of process settings and other details. An SD card was used to transport the file to the resin 3D printer once it had been sliced and formatted for printing.

A resin-based 3D printer was used to create nanocomposite specimens in accordance with preset process parameter settings. With parameter ranges described in Table 1, a total of 20 specimens were produced under the process circumstances shown in Figure 2.

Table 1: *Requirement for single-objective optimization of Shore-D Hardness*

Parameter	Units	Level 1	Level 2	Level 3
D:Exposure time	seconds	3	4	5
E:Slice height	microns	20	30	40
F:Post curing time	minutes	10	20	30

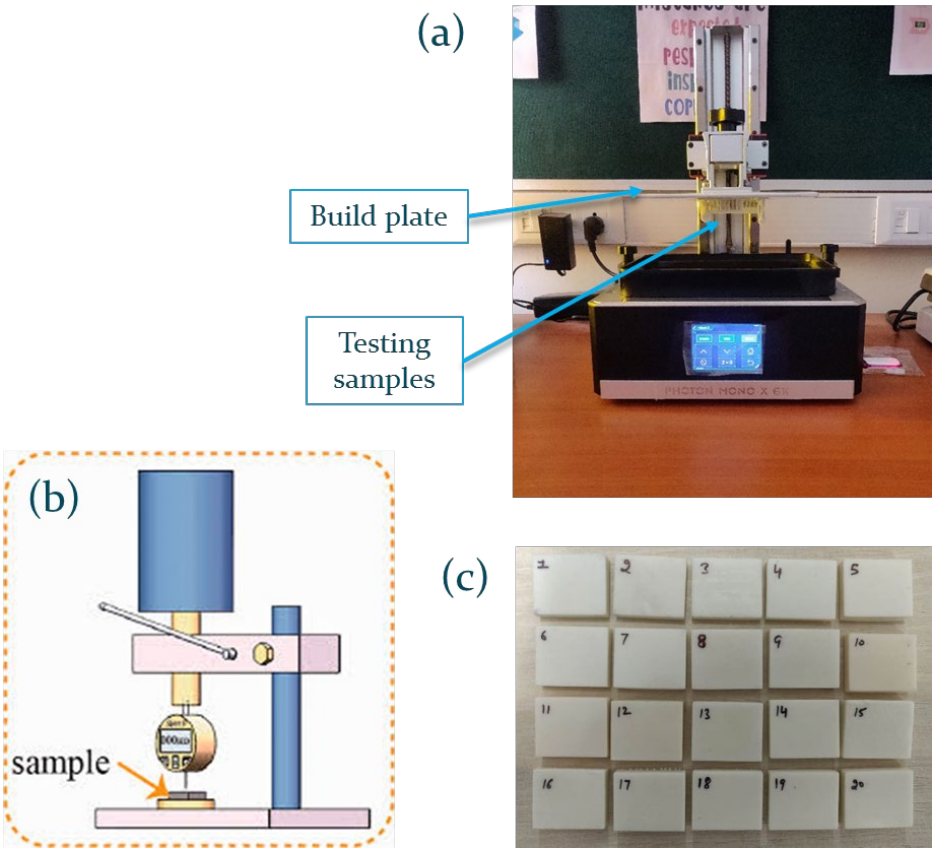

Figure 2: *(a) 3D printing setup, (b) Shore-D hardness test setup, (c) testing specimens*

The durometer setup used to determine the hardness of the manufactured samples is shown in Figure 2(a). At several positions along the measuring line, the samples were put beneath the indenter for 10 seconds, and the mean value was determined using these measurements. A scale of 0 to 100 was used to measure the hardness; higher numbers denoted greater material hardness. The hardness was calculated and given in SHD. Table 2 provides a summary of the data gathered during the experiments.

II. Statistical Analysis

The information obtained from the trial outcomes was assessed using Design-Expert 13. Centre composite design was used to tabulate the combination of input variables at their different levels. Numerous quantitative characteristics, such as coefficients of deviation, lack of fit, and computed and shifted multiple correlation coefficients, were carefully analysed among several polynomial models in order to choose the most suitable model with $p<0.05$. To understand how input variables impacted replies, interaction, factor, and 3D graphs were created using the DX-13 tool.

III. Results and Discussion

A resin 3D printer was used to create and test twenty specimens. Table 2 displays the computed hardness findings. Using twenty permutations of three input elements and the hardness of the generated nanocomposite, a mathematical model was created. Equation 1 shows the mathematical connection that was established by calculating the shore hardness coefficient values.

$$\text{Hardness} = 88.6546 + 1.17188D - 0.109375E + 0.924417F + 0.15625DE - 0.09375DF + 0.03125EF - 1.34653D^2 - 0.627781E^2 - 1.41743F^2 \quad (1)$$

Table 2: *Experimental results for Shore-D Hardness*

Run	Factor 1	Factor 2	Factor 3	Response 1
	D:Exposure Time (second)	F:Slice Height (micron)	F:Post Curing Time (min)	Shore Hardness (SHD)
1	5	20	30	87.00
2	4	30	20	88.50
3	4	30	20	88.75
4	5	20	10	85.50
5	6	30	20	85.75
6	3	20	10	83.25
7	4	30	20	88.75
8	5	40	30	87.25
9	2	30	20	81.00
10	4	30	40	85.00
11	4	30	20	88.50
12	4	30	20	88.75
13	4	30	20	88.75
14	4	30	10	86.50
15	3	40	30	84.75
16	3	20	30	85.25
17	3	40	10	82.75
18	5	40	10	85.50
19	4	50	20	86.00
20	4	10	20	86.50

The model's adequacy was determined by an ANOVA test on the confidence level of 95%, with findings shown in Table 5.8. The findings showed the model's significance and could be utilized to

determine the developed nanocomposite's shore hardness without performing real experiments. The model's p-value is lower than 0.0001, indicating its statistical relevance and significance. In this case, D, E, F, DE, D^2, E^2, F^2 are significant model terms. The model's R^2 is 0.99.7, indicating that approx. The input factors explain 99.7 % of the variation in the shore hardness. The model's adequate precision is 62.95, representing the significance of the signal. The C.V. for this model also signifies an acceptable level of data dispersion.

Table 3: *ANOVA test results for Shore D Hardness*

Source	Sum of Squares	df	Mean Square	F-value	p-value	
Model	91.52	9	10.17	337.29	< 0.0001	significant
D-Exposure time	21.97	1	21.97	728.79	< 0.0001	
E-Slice height	0.1914	1	0.1914	6.35	0.0304	
F-Post curing time	8.98	1	8.98	297.95	< 0.0001	
DE	0.1953	1	0.1953	6.48	0.0291	
DF	0.0703	1	0.0703	2.33	0.1577	
EF	0.0078	1	0.0078	0.2591	0.6218	
D^2	46.89	1	46.89	1555.36	< 0.0001	
E^2	10.19	1	10.19	338.08	< 0.0001	
F^2	26.27	1	26.27	871.27	< 0.0001	
Residual	0.3015	10	0.0301			
Lack-of-Fit	0.2182	5	0.0436	2.62	0.1572	not significant
Pure-Error	0.0833	5	0.0167			
Cor Total	91.83	19				

Figure 3 presents the variation between experimental and predicted hardness values, demonstrating that the predicted values agree with the experimental ones. Figure 4 illustrates the influence of exposure time, slice height and post curing time on the hardness of the nanocomposite. The results show that the developed composite exhibits lower hardness at a shorter exposure time. As the exposure time increases, the hardness improves significantly, reaching its peak at 4.5 minutes of exposure. Once this point is exceeded, a slight reduction in hardness occurs. This decrease may be attributed to potential changes in the material's microstructure that could occur after an optimal exposure time is exceeded.

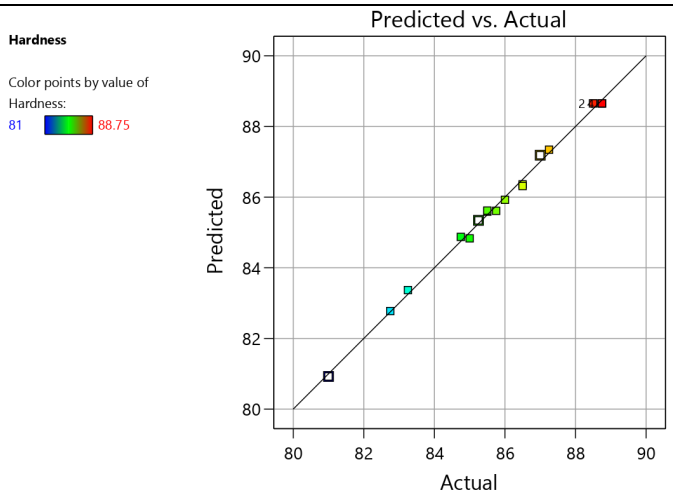

Figure 3: *Predicted v/s actual values for shore – D hardness*

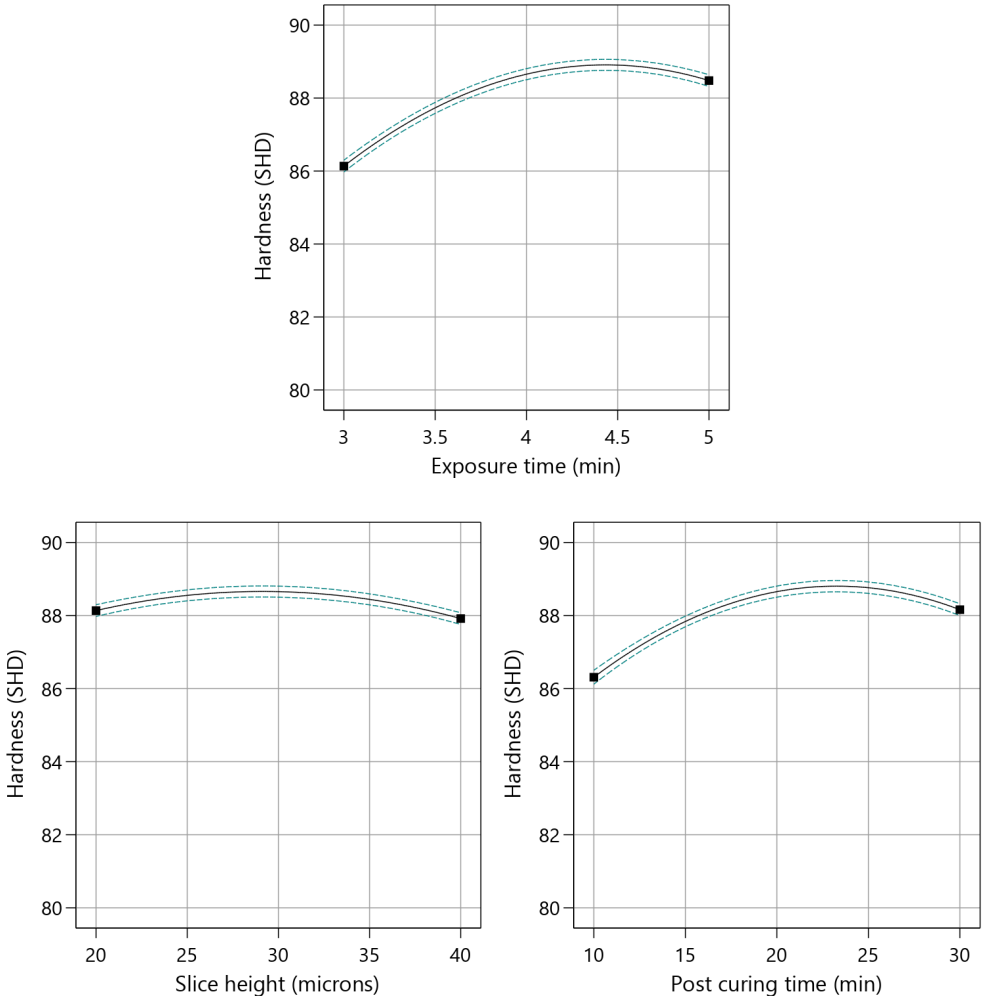

Figure 4: *Effect of process parameter on shore D hardness (a) hardness v/s exposure time, (b) hardness v/s slice height and, (c) hardness v/s post curing time*

The findings indicate a gradual enhancement in hardness with slice height, peaking at 27 microns. Beyond this height, a steady decline in hardness is observed. The data reveal that the composite

exhibits lower hardness at shorter PCT. As the PCT increases, the hardness improves significantly, reaching its highest value at 24 minutes. Beyond this point, a slight decline in hardness is observed. This trend may be due to the continued polymerization and cross-linking during post-curing, which strengthens the material. However, extended post-curing time could lead to over-curing or excessive brittleness, resulting in slightly reduced hardness.

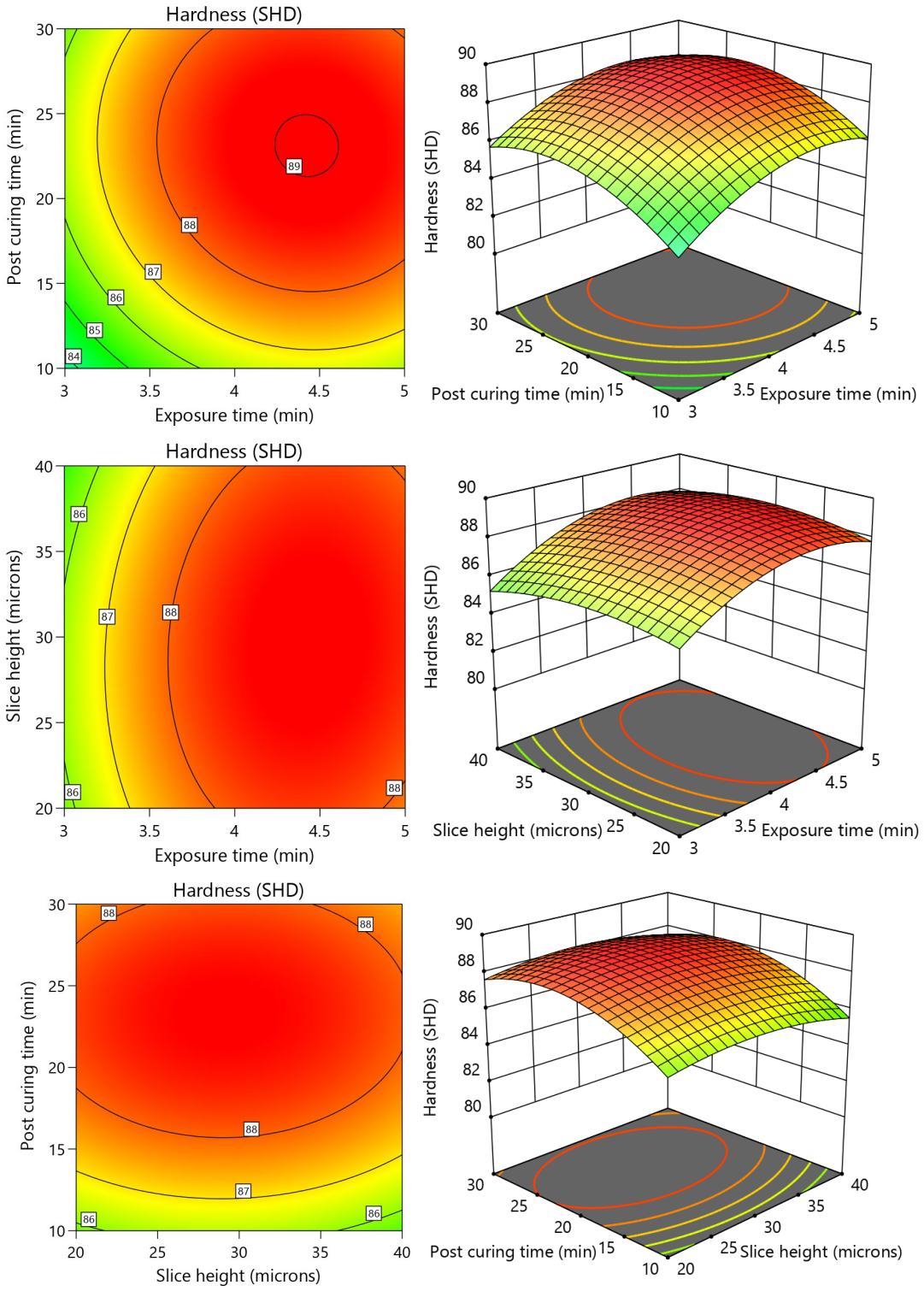

Figure 5: *Interaction effects of exposure time, layer height and post-curing time on the Shore Hardness of SS 316L reinforced PMMA*

The influence of combined parameters on the Shore Hardness of SS 316L reinforced PMMA is illustrated through the plots in Figure 5. The shore hardness of the composite was low at lower PCT and ET. The maximum shore hardness was observed at an exposure time of 4.3 – 4.7 minutes and the post-curing time between 23-25 minutes. At lower exposure times, the composite showed reduced shore hardness, irrespective of slice height. The highest shore hardness was observed at higher exposure time, between 4 - 5 minutes, regardless of the slice height. Figure 6.41 depicts the interaction effect of PCT and slice height on the shore hardness of the SS 316L reinforced PMMA composite. The shore hardness of the composite was low at lower post-curing time (10 to 17 minutes), regardless of slice height. The highest shore hardness was achieved at the post-curing time of 18–30 minutes and slice height between 20-40 microns.

The criteria for different process parameters in single-objective optimization of response parameter, i.e., shore hardness, is shown in Table 4. The goal is to maximize the shore hardness of the SS 316 L reinforced PMMA composite within the specified range of input parameters.

Table 4: *Requirement for single-objective optimization of shore D hardness*

Name	Goal	Lower Limit	Upper Limit	Lower Weight	Upper Weight	Importance
D:Exposure time	is in range	3	5	1	1	***
E:Slice height	is in range	20	40	1	1	***
F:Post curing time	is in range	10	30	1	1	***
Hardness	maximize	81	88.75	1	1	***

The response and all factors were given equal importance, and specific goals were set for each parameter. The response surface methodology (RSM) generated a total of 100 possible solutions, from which the optimal solution was selected based on maximum desirability and practical feasibility. The optimal combination of input parameters exposure time, layer height, and post-curing time, i.e., is determined to be 4.74 seconds, 30.7 microns, and 23.20 minutes, respectively. The corresponding optimal value of response parameters was obtained as follows: Shore hardness – 88.90 SHD. These results are visually represented by the ramp function graphs in Figure 6. The model was validated using the optimal process parameters from the RSM-generated model. Three specimens were fabricated for each condition, and experimental results showed a maximum error of less than 1.8%, confirming the model's accuracy and reliability.

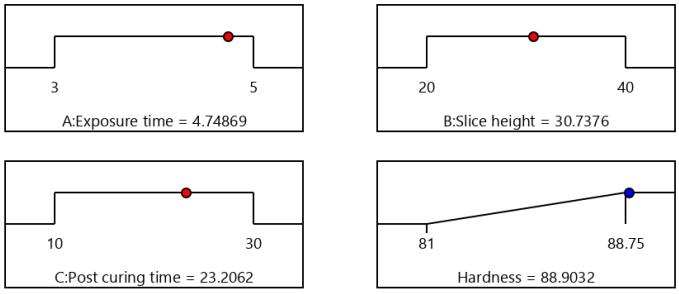

Figure 6: *Ramp function graphs for single-objective optimization of Shore D Hardness*

IV. Conclusion

The hardness of resin 3D-printed parts reinforced with 316L-PMMA nanocomposite is examined in this work under various process conditions. The findings show that changes in process parameters have a major impact on hardness characteristics, with exposure and post-curing times appearing as important variables. Up to an ideal threshold, the hardness rises as exposure duration increases. The model's robustness and dependability are confirmed by validation using the Response Surface Methodology (RSM), which produces an R^2 value of 0.997. With a maximum shore D hardness of 88.90 SHD at an exposure period of 4.74 seconds, a layer height of 30.7 microns, and a post-curing time of 23.2 minutes, RSM optimisation efficiently maximises the hardness.

References

[1] Shahrubudin, N., Lee, T. C. and Ramlan, R. (2019). An overview on 3D printing technology: Technological, materials, and applications. *Procedia Manufacturing*, 35:1286–1296.

[2] Seprianto, D., Putra, D. P., Yanis, M. and Basri, H. (2021). Optimization of Production Process Parameters of DLP Type 3D Printer Design for Product Roughness Value. *Proceedings of the 4th Forum in Research, Science, and Technology*, 7:179–183.

[3] Tsolakis, I. A., Papaioannou, W., Papadopoulou, E., Dalampira, M. and Tsolakis, A. I. (2022). Comparison in terms of accuracy between DLP and LCD printing technology for dental model printing. *Dentistry Journal*, 10(10): 181.

[4] Liu, Y., Liang, L., Rajan, S. S., Damade, Y., Zhang, X., Mishra, K., Qu, L. and Dubey, N. (2024). Recent advances in additive manufacturing for tooth restorations. *Applied Materials Today*, 39:102275.

[5] Rindfleisch, A., O'Hern, M. and Sachdev, V. (2017). The digital revolution, 3D printing, and innovation as data. *Journal of Product Innovation Management*, 34(5):681-690.

[6] Jockusch, J. and Özcan, M. (2020). Additive manufacturing of dental polymers: An overview on processes, materials and applications. *Dental materials journal*, 39(3): 345-354.

[7] Punia, U. and Garg, R. K. (2024). Reinforcing dental restoration material PMMA with SS 316L nanoparticles for mechanical performance analysis. *Progress in Additive Manufacturing*, 10, 3003–3014.

[8] Omondi, O. B., Arroyan, Y. N., Onyango, B., Kong, L., Wang, G. and Ye, Z.(2024). Revolutionizing healthcare: Emerging frontiers in 3D bioprinting of tissues and organs. *European Polymer Journal*, 217.

[9] Punia, U., Dhull, S., Habeeb, A., Antil, E., Dahiya, D., Gupta, D. and Ahlawat, A. (2025). Adopting additive manufacturing: Spotlight on sustainability and material utilization. *Green Materials*, 1-11.

[10] Ibrahim, S. A., Lafta, S. H. and Hussain, W. A. (2021). Impact strength of surface treated SS316L wires reinforced PMMA. *Journal of the Mechanical Behavior of Materials*, 30(1): 272-278.

[11] Punia, U. and Garg, R. K. (2024). Enhancing mechanical performance of 3D printable PMMA resin through strategic incorporation of SS 316 L nanoparticles for dental applications. *International Journal on Interactive Design and Manufacturing (IJIDeM)*, 18(8): 6317-6332.

[12] Dhanunjayarao, B. N. and Naidu, N. S. (2022). Assessment of dimensional accuracy of 3D printed part using resin 3D printing technique. *Materials Today: Proceedings*, 59: 1608-1614.

[13] Hwangbo, N. K., Nam, N. E., Choi, J. H. and Kim, J. E. (2021). Effects of the washing time and washing solution on the biocompatibility and mechanical properties of 3D printed dental resin materials. *Polymers*, 13(24): 4410.

[14] Guerra, A. J., Lammel-Lindemann, J., Katko, A., Kleinfehn, A., Rodriguez, C. A., Catalani, L. H., Becker, M.L., Ciurana, J. and Dean, D. (2019). Optimization of photocrosslinkable resin components and 3D printing process parameters. *Acta biomaterialia*, 97:154-161.

[15] Yang, Y., Zhou, Y., Lin, X., Yang, Q. and Yang, G. (2020). Printability of external and internal structures based on digital light processing 3D printing technique. *Pharmaceutics*, 12(3): 207.

[16] Li, S., Yuan, S., Zhu, J., Wang, C., Li, J. and Zhang, W. (2020). Additive manufacturing-driven design optimization: Building direction and structural topology. *Additive Manufacturing*, 36: 101406.

[17] Zaldivar, R. J., Witkin, D. B., McLouth, T., Patel, D. N., Schmitt, K. and Nokes, J. P. (2017). Influence of processing and orientation print effects on the mechanical and thermal behavior of 3D-Printed ULTEM 9085 Material. *Additive Manufacturing*, 13: 71-80.

[18] Schittecatte, L., Geertsen, V., Bonamy, D., Nguyen, T. and Guenoun, P. (2023). From resin formulation and process parameters to the final mechanical properties of 3D printed acrylate materials. *MRS Communications*, 13(3): 357-377.

[19] Wiese, M., Thiede, S. and Herrmann, C. (2020). Rapid manufacturing of automotive polymer series parts: A systematic review of processes, materials and challenges. *Additive Manufacturing*, 36: 101582.

[20] Bardelcik, A., Yang, S., Alderson, F. and Gadsden, A. (2021). The effect of wash treatment on the mechanical properties and energy absorption potential of a 3D printed polymethyl methacrylate (PMMA). *Materials Today Communications*, 26: 101728.